STEM CELLS AND DEVELOPMENT
Volume 23, Number 17, 2014

DOI: 10.1089/scd.2013.0639

Stable Methylation at Promoters Distinguishes Epiblast Stem Cells from Embryonic Stem Cells and the In Vivo Epiblasts

Anne-Clémence Veillard,[1] Hendrik Marks,[2] Andreia Sofia Bernardo,[3,4] Luc Jouneau,[1] Denis Laloë,[5] Laurent Boulanger,[1] Anita Kaan,[2] Vincent Brochard,[1] Matteo Tosolini,[1] Roger Pedersen,[4] Henk Stunnenberg,[2] and Alice Jouneau[1]

Embryonic Stem Cells (ESCs) and Epiblast Stem Cells (EpiSCs) are the in vitro representatives of naïve and primed pluripotency, respectively. It is currently unclear how their epigenomes underpin the phenotypic and molecular characteristics of these distinct pluripotent states. Here, we performed a genome-wide comparison of DNA methylation between ESCs and EpiSCs by MethylCap-Seq. We observe that promoters are preferential targets for methylation in EpiSC compared to ESCs, in particular high CpG island promoters. This is in line with upregulation of the de novo methyltransferases Dnmt3a1 and Dnmt3b in EpiSC, and downregulation of the demethylases Tet1 and Tet2. Remarkably, the observed DNA methylation signature is specific to EpiSCs and differs from that of their in vivo counterpart, the postimplantation epiblast. Using a subset of promoters that are differentially methylated, we show that DNA methylation is established within a few days during in vitro outgrowth of the epiblast, and also occurs when ESCs are converted to EpiSCs in vitro. Once established, this methylation is stable, as ES-like cells obtained by in vitro reversion of EpiSCs display an epigenetic memory that only extensive passaging and sub-cloning are able to almost completely erase.

Introduction

Two kinds of pluripotent stem cells can be captured ex vivo from the mouse embryo: embryonic stem cells (ESCs) are derived from the inner cell mass (ICM) of the blastocyst, whereas epiblast stem cells (EpiSCs) are isolated from the late epiblast of postimplantation embryos. Although both express the core triad of transcription factors Oct4/Sox2/Nanog, some other pluripotency factors identified in ESCs are absent in EpiSCs, such as *Esrrb*, *Klf4*, *Rex1/Zfp42*, and *Dppa3/Stella* [1,2]. Moreover, transcriptome comparisons have indicated that EpiSCs may be closer to the postimplantation epiblast, whereas ESCs share more characteristics with ICM cells [3]. Indeed, EpiSCs express late epiblast markers such as *Nodal*, *Fgf5*, *Brachyury* (*T*), or *Cer1*, which are low or absent in ESCs [4]. These contrasting signatures suggest these cell types represent two different states of pluripotency, naïve for ESCs and primed for EpiSCs [5]. In contrast to ESCs, EpiSCs are unable to form chimeras following injection into blastocysts [3,6]. However, they can contribute, at least to some extent, to embryo development if injected in the postimplantation epiblast [7].

Different signaling pathways control self-renewal of these pluripotent states: ESCs require LIF and BMP4, while EpiSCs are dependent on FGF2 and Activin/Nodal [3,8]. By switching between the appropriate culture conditions for each cell type, ESCs can be readily converted into EpiSCs, whereas EpiSCs can also be reverted into naïve ES-like cells in vitro albeit with low efficiencies [9–11]. Such interconversion abilities provide new avenues to study the relationships between the two states of pluripotency and have elicited the notion of an ''epigenetic barrier'' separating ESCs from EpiSCs, since reprogramming EpiSCs into naïve ESCs is an inefficient and long process. In particular, de novo DNA methylation, which takes place during epiblast development [12,13], may be a constituent of this barrier as it is in somatic cell reprogramming [14]. De novo DNA methylation is catalyzed by the de novo methyltransferase 3

[1]INRA, UMR1198 Biologie du Développement et Reproduction, Jouy-en-Josas, France.
[2]Department of Molecular Biology, Faculty of Science, Radboud Institute for Molecular Life Sciences (RIMLS), Radboud University, Nijmegen, The Netherlands.
[3]Systems Biology Division, MRC National Institute for Medical Research, Mill Hill, London, United Kingdom.
[4]Laboratory for Regenerative Medicine, Department of Surgery, University of Cambridge, Cambridge, United Kingdom.
[5]INRA, UMR GABI, Jouy-en-Josas, France.

(Dnmt3) enzymes [15]. Three have been isolated in mammals: Dnmt3a and Dnmt3b are catalytically active, while Dnmt3l, is a cofactor for both. In the epiblast, Dnmt3b is the first to be expressed at E3.5 while Dnmt3a expression starts 1 day later [16–18]. Dnmt3l is expressed transitorily in the epiblast, between E4.5 and E6.5 [16,18]. The ICM of E3.5 blastocyst is globally hypomethylated, while a massive wave of de novo methylation occurs between the epiblast stages E3.5 and E6.5 [13]. Interestingly, the methylome of ESC is shaped by their culture conditions: ESCs cultured in the presence of the two kinase inhibitors, inhibiting Gsk3 and FGF signaling, respectively, are globally hypomethylated and resemble ICM cells. ESCs cultured using serum conditions display a methylation profile more similar to that of the early postimplantation epiblast [12,19,20]. In contrast, little is known about the methylome of EpiSCs. Quantitatively, the global level of 5-methylcytosine in EpiSCs was found to be similar to that of ESC cultured in serum [20,21]. A recent study by Senner et al. [21] showed that four types of stem cells derived from the mouse embryo, either extraembryonic or embryonic, contained a unique DNA methylation signature. However, an in-depth comparison of the methylome of ESCs and EpiSCs is currently lacking.

Here, we compare the patterns of DNA methylation in EpiSCs and ESCs and observed a clear bias toward promoter-associated hypermethylation in EpiSCs. By following the kinetics of methylation during ESC to EpiSC conversion, we show that de novo methylation seems to occur very rapidly and concomitant to the molecular switch. Conversely, reversion of EpiSC into ES-like cells shows that the reprogramming of methylation at the promoters is very slow and incomplete, suggesting the persistence of an epigenetic memory. Finally, a comparison of EpiSCs and late epiblast cells reveals that the in vitro and ''in embryo'' cells show a remarkably different promoter methylation profile.

Materials and Methods

Preparation of samples for sequencing

MethylCap. Genomic DNA was sonicated to generate 300 bp fragments on average. MethylCap was performed using the IP-STAR robot (Diagenode) as described before [22]. In short, 1 μg DNA was incubated with paramagnetic beads coated with the MBD domain of MeCP2 fused to GST. After washing with 200, 400, and 500 mM NaCl, the bound methylated DNA was eluted in two fractions using 600 and 800 mM NaCl, respectively. Twenty nonogram of DNA eluates was prepared for sequencing.

Double-stranded cDNA synthesis. Total RNA was isolated with TRIzol (Invitrogen) according to the manufacturer's recommendations. One hundred microgram total RNA was subjected to two rounds of poly(A) selection (Oligotex mRNA Mini Kit; QIAGEN), followed by DNaseI treatment (QIAGEN). About 100–200 ng mRNA was fragmented by hydrolysis (5× fragmentation buffer: 200 mM Tris acetate, pH8.2, 500 mM potassium acetate, and 150 mM magnesium acetate) at 94°C for 90 s and purified (RNAeasy Minelute Kit; QIAGEN). cDNA was synthesized using 5 μg random hexamers by Superscript III Reverse Transcriptase (Invitrogen). Double-strand cDNA synthesis was performed in second strand buffer (Invitrogen) according to the manufacturer's recommendations and purified (Minelute Reaction Cleanup Kit; QIAGEN).

Sequencing

DNA or cDNA samples were prepared for sequencing by end repair of 20 ng DNA as measured by Qubit (Invitrogen). Adaptors were ligated to DNA fragments, followed by size selection (~300 bp) and 14 cycles of PCR amplification. Integrity of DNA libraries was confirmed by running the products on a Bioanalyzer (BioRad). Cluster generation and sequencing (36 bp) was performed with the Illumina Genome Analyzer IIx (GAIIx) (MethylCap-seq) or HiSeq (RNA-seq) platform according to standard Illumina protocols. Initial data processing, base calling, and alignment to the mouse reference genome was performed using the Illumina Analysis Pipeline allowing one mismatch. Only tags aligning to one position on the genome were considered for further analysis. For RNA-seq, further analysis was performed with the 36 bp aligned sequence. For MethylCap-seq, the uniquely mapped sequence reads were directionally extended to 300 bp, the estimated median length of the original DNA library. If multiple tags were mapped on the same genomic position, only one was included for further analysis. Mapped reads from the initial 600 and 800 mM NaCl eluate libraries were combined. For both RNA-seq and MethylCap-seq data were converted to Browser Extensible Data files for downstream analysis. To compensate for differences in sequencing depth and mapping efficiency among samples, the total number of unique reads of each sample was uniformly equalized relative to the sample with the lowest number of sequence reads, allowing quantitative comparisons. Wiggle (WIG) files for viewing the data in the UCSC Genome Browser were generated from the normalized files. All sequencing analyses were conducted based on the Mus musculus NCBI m37 genome assembly (MM9; assembly July 2007). Supplementary Table S1 summarizes the sequencing output.

MethylCap-seq analyses

Peak calling. Data analysis was performed using in-house generated scripts written in LINUX shell, Perl, and R. Enriched regions (peaks) were called on the basis of a Poisson distribution of overlapping sequence reads within a dynamic window. A false discovery rate (FDR) was calculated relative to the total covered sequence, and peaks with an FDR of $\leq 1 \times 10^{-6}$ were selected. All peaks from the four samples (three EpiSCs and one ESC) were merged. Per sample, the number of normalized sequence reads overlapping each region (peak) of interest was calculated, which is referred to as read density and used as a measure of DNA methylation.

Annotation. Methylated peaks were annotated according to their localization in the genome, as intron, exon, promoter (−900 to +400 bp around the gene start), or intergenic based on the Ensembl release 66 (MM9 assembly). As peaks often span different genomic regions, we used the summit genomic coordinate of each peak as representative. Due to the presence of overlapping transcripts in the mouse genome, about 5% of the peaks were annotated to multiple genes. Therefore, peaks were annotated with (at least one) gene name and sequence type (exon, intron, and promoter). Nonassigned peaks were considered as intergenic.

Gene Ontology and KEGG analysis was performed using DAVID (http://david.abcc.ncifcrf.gov) [23,24]. Further data analysis was performed using IPA (Ingenuity® Systems, www.ingenuity.com).

RNA-seq analysis

To obtain RNA-seq gene expression values (RPKM), we used Genomatix (www.genomatix.de).

Statistical analysis of MethylCap seq data

Read counts for all peaks and transcripts were normalized using the normalization procedure used in the Bioconductor package ''DESeq'' [25]. We used these normalized counts to perform a hierarchical clustering analysis of methylome samples using the distance function 1-*c*, where *c* is the correlation coefficient, and the Ward linkage method.

To study the relation between DNA methylation and expression, we built a reduced dataset where methylation peaks corresponding to promoters were combined with read counts for the corresponding transcripts. The following thresholds were used for including genes: methylation read density >0 for either the ESC sample or for at least 2 EpiSC samples.

After log2 transformation of normalized counts, we used the R package ''flexclust'' [26] to group methylation and expression profiles in clusters. Only clusters having at least 10 profiles and a Pearson correlation coefficient greater than 0.9 (with the center profile of the cluster; radius–that is maximum distance to the cluster center profile = 0.1), were included.

Cell lines and culture conditions

Derivation of the 129S2 ESC line was performed as previously described [27]. The rESCs (129S2 rESCs) and ESCs (129S2 ESCs, 129B6 ESCs, and R1) were grown on irradiated mouse embryonic fibroblasts in medium containing DMEM with either 15% serum or (for 129S2 ESCs) 20% KSR (Invitrogen), 0.1 mM β-mercaptoethanol and 1,000 U/mL LIF (ESGRO; Millipore) and plated feeder-free on gelatin-coated dishes for two passages before collection. EpiSCs (129S2 EpiSCs, EpiSC1, 2, and 3 described in Maruotti, 2010 and 129B6 EpiSCs) and cEpiSCs (129S2 cEpiSCs) were grown in serum-free medium (CDM) with FGF2 (12 ng/mL; R&D) and Activin A (20 ng/mL; R&D) on serum-coated dishes as previously described [3]. Conversion of 129S2 ESCs was performed as previously described [9,28]. In summary, the ESCs were trypsinized and 1.5×10^6–3×10^6 cells were seeded in 35 mm, serum-coated dishes in CDM + FGF2 and Activin. At day 4, cells were detached with collagenase-II (Sigma) and replated without dilution. This first passage promotes the appearance of flat colonies with typical EpiSC morphology. Converted cells were then cultured for several passages before harvesting. For reversion, EpiSCs were passaged onto mouse irradiated feeders in the presence of ESC medium as described. After 7 days, cells were trypsinized and passaged as ESCs for at least five passages.

Epiblast dissection

E6.5 and E7 epiblasts were dissected from CDI mouse embryos in Flushing and Handling Medium (FHM). The embryonic region was cut out from extra-embryonic tissue and incubated for 10 min in FHM containing 0.1% Trypsin (Type II, Sigma) and 2.5% Pancreatin (Sigma). The epiblast was then isolated using glass needles and either snap-frozen or plated in four-well plate in CDM supplemented with Activin and Fgf2 for EpiSC derivation as described [29].

Real-time PCR analysis

Total RNA was extracted and reverse-transcribed with Superscript III (Invitrogen). Real-Time PCR were carried out using SybrGreen mix (Qiagen) on a Step One Plus thermal cycler (Applied Biosystem) and repeated thrice on independent experiments and/or cell lines. Data were normalized using the geometric mean of *Hprt* and *Pbgd* using Qbase software (Biogazelle). Primers used are listed in Supplementary Table S2.

Western-blot analysis

Cellular samples were lysed in 3 × Laemli-SDS buffer. The polypeptides were separated through 4%–12% Bis- Tris Gel NuPage electrophoresis and transferred onto a polyvinylidene difluoride membrane (Hybond-P PVDF; Amersham). After blocking with 1/1,000 Tween 20-PBS (PBS-T) containing 4% (w/v) nonfat dried milk, the membranes were incubated with primary antibodies overnight at 4°C. Antibodies used were as follows: mouse monoclonal anti-Dnmt3b (Abcam; 1/1,500 dilution) or anti-Dnmt3a (Active Motif; 1/1,000 dilution). The membranes were washed thrice with PBS-T, incubated with a peroxidase-conjugated anti-mouse antibody and washed again. Peroxidase activity was measured using the ECL-Plus Western Blot detection system (Amersham) and a LAS 1000 camera (Fuji). The membranes were incubated with an anti-Actin antibody for loading control. Band intensities were quantified using ImageJ software (http://imagej.nih.gov/ij/index.html) and normalized using Actin.

DNA methylation analysis by bisulfite sequencing

Genomic DNA was purified using DNA extraction kit (Promega) according to the manufacturer's instructions. For epiblast DNA, pools of seven (E6.5) or three (E7) epiblasts were digested by proteinase K in lysis saline buffer and DNA was extracted using NaCl/EtOH precipitation.

Bisulfite conversion was performed as previously described [30] on 1 μg of genomic DNA for the cells, or all DNA obtained from epiblasts. Regions of interest were then amplified by PCR using the KAPA HiFi HotStart Uracil + mix (Clinisciences) using primers listed in Supplementary Table S2. The PCR program was as follows: 5 min at 95°C followed by 40 cycles of 20 s at 98°C, 30 s at 60°C, and 15 s at 72°C, with a final extension of 5 min at 72°C. PCR products were directly sequenced or subcloned into pGEMTeasy vector (Promega). Clones were amplified by PCR using the Platinum taq polymerase (Invitrogen) with 5% DMSO at 95°C 15 min followed by 35 cycles of 30 s at 95°C and 3 min at 64°C with a final extension 10 min at 64°C. PCR products of the expected size and quantity were sequenced and analyzed using BiQ Analyzer software [31].

Processing of publicly available datasets for methylation and expression in the epiblast

For comparisons with epiblast methylation, we used profiles of GEO series GSE22831 [12]. Oligo sequences of NimbleGen Mouse Promoter Array (GPL9485) were mapped to the MM9 genome assembly using bowtie2 with a maximum of three mismatches. Sequences mapping on multiple loci in the genome were discarded. For the methylation profiles of the three epiblast (E6.5) replicates within GSE22831 we computed the average log-ratios per NimbleGen probe. For each promoter regions covered by our Methylcap dataset and by the NimbleGen probes (only regions containing ≥ 5 probes were included), we computed the number of probes, the percentage of probes having an average log-ratio larger than 0.5 and the average log-ratios of all probes within the promoter. The classification of promoters was according to Borgel et al. [12]: low or no methylation (log2ratio < 0.3), or highly methylated (log2-ratio > 0.4).

To determine expression levels for genes showing hypermethylated promoters in EpiSCs, we used profiles within GEO series GSE4622 [32], that is, the microarray data for epiblast at prestreak (two replicates) and mid-streak (three replicates) stages (same stages as used for EpiSC derivation, bisulfite sequencing, and RT-qPCR in this study). A gene was considered to be expressed in one sample in case of a detection P-value < 0.05, and considered to be expressed in the epiblast if detected in at least four out of five samples.

Accession numbers

The GEO accession number for the MethylCaq-seq and RNA-seq data for EpiSCs reported in this article is GSE47793. The GEO accession numbers for the previously generated MethylCap-seq and RNA-seq profiles of ESCs are GSE31343 and GSE23943, respectively [33,34]. Raw sequencing data of MeDIP-Seq from Senner et al. [21] were downloaded from the EBI European Nucleotide Archive (ENA) accession number PRJEB4263.

Results

DNA methylation profiles of ESCs and EpiSCs

To investigate the DNA methylome of ESCs and EpiSCs at a genome-wide scale, we applied MethylCap-sequencing. This method involves capture of methylated DNA using the MBD domain of MeCP2, followed by parallel sequencing of the captured DNA. In comparison to other genome-wide DNA methylation profiling methods, MethylCap-seq stands out for its robustness, sensitivity, and costeffectiveness [22]. MethylCap-seq was performed on three EpiSC lines (EpiSC1 and 3, male; EpiSC2, female) derived from fertilized B6D2F1 embryos and characterized in [29]. We compared these new profiles with an ESC line (male, E14Tg2a) [33]. Overall a total of 90,474 methylated regions were identified, with a median length of 2,034 bp. These regions are distributed across all chromosomes (Supplementary Fig. S1A). Furthermore, the read density distribution plots of all enriched regions, representative for the level of methylation at the individual loci, in either ESCs or EpiSCs were well overlaid (Supplementary Fig. S1B). This suggests that, overall, DNA methylation is similar in ESCs and EpiSCs at a global level in accordance with Senner et al. [21].

Methylated regions were annotated according to their genomic localization: intergenic, exonic, intronic, and promoter regions. The partition of the methylated regions into these categories was the same in both pluripotent cell types, with an overrepresentation of intragenic methylation compared with the genomic background distribution within the nonrepetitive portion of the genome (Supplementary Fig. S1C). Despite these similarities between ESC and EpiSC methylation, hierarchical clustering clearly shows that the ESC methylome is distinct from that of EpiSCs (Fig. 1A). To get insight into this distinction, we plotted the read density distribution of the regions according to their genomic localization and observed that the read distribution of regions annotated as promoters was shifted toward higher read densities (ie, higher methylation) in EpiSCs compared with ESCs (Fig. 1B). Classifying promoters according to their CpG density [35], high-, intermediate-, and low-CpG content promoters (HCPs, ICPs, and LCPs, respectively), the shift revealed that the higher methylation in EpiSCs is mainly present in HCPs (Fig. 1C), and not so much in ICPs and LCPs.

Relation of promoter methylation to gene expression

To understand the functional importance of methylation differences in the promoters, we first examined the statistic correlation between DNA methylation at promoters and gene expression in ESCs and EpiSCs. We generated transcriptome profiles of the same three EpiSC lines by RNA-seq and used previously generated RNA-Seq data for the E14 ESC line used in this study [34]. We determined the correlation coefficients between promoter methylation and expression of the corresponding genes (Fig. 2A), followed by a principal component analysis performed on the matrix of these correlations (Supplementary Fig. S2A). Overall, there is a limited variability within EpiSC lines, exhibiting high positive correlations between methylation peaks (0.61–0.85). It is noteworthy that these correlation coefficients are lower between the male lines (EpiSC1 and EpiSC3) and the female one (EpiSC2), reflecting the presence of an inactivated and highly methylated X-chromosome in the female. In addition, although gene expression of the different EpiSC and ESC lines is closely related (between 0.9 and 0.99 correlation), lower correlations were observed between ESC and EpiSC methylation (0.31–0.57). Lastly, an anti-correlation between gene expression and methylation peaks was observed (between -0.08 and -0.35).

To gain more insight in the anti-correlation between gene expression and DNA methylation we performed quality threshold clustering (QT-Clust; Supplementary Fig S2B), summarized in Fig. 2B. Fifty-eight percent of the genes present in the combined datasets followed pattern 1, that is, showed both high promoter methylation and low expression. Conversely, 29% of the genes followed the opposite pattern (pattern 2), characterized by low promoter methylation and high expression. An example of a gene following pattern 1 is shown on Fig. 2C. However, a few genes seem to escape from methylation-induced repression, as illustrated with *Car4* (Supplementary Fig. S2C). Interestingly, pattern 3

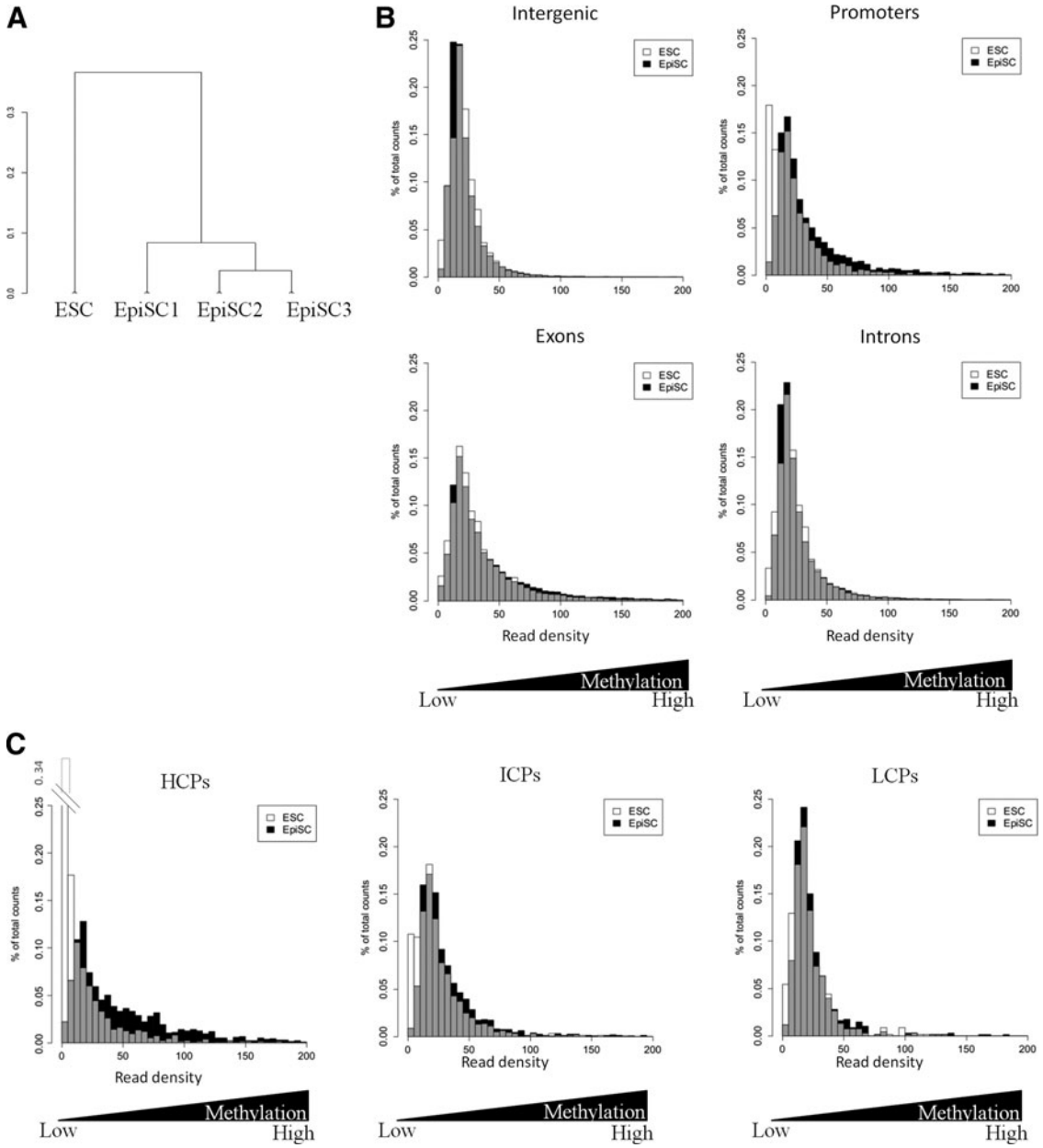

FIG. 1. Global analysis of DNA methylation in embryonic stem cell (ESC) and epiblast stem cells (EpiSC) lines. **(A)** Hierarchical clustering of methylation profiles, based on a Pearson's correlation distance matrix. **(B, C)** Distribution of read density for ESCs and EpiSCs (mean of the three cell lines) in each genomic category **(B)** and in promoters annotated as high (HCP), intermediate (ICP), or low (LCP) CpG content **(C)**. Bars for EpiSC are in *white*, bars for ESC in *black*, the overlay in *gray*.

characterized by high methylation only in the female EpiSC line (EpiSC2) contained mostly genes located on chromosome X (90%), in agreement with the presence of an inactivated X in this female line. This specificity of the EpiSC2 line probably explains the weaker anti-correlation (-0.08) compared with the others (-0.23 to -0.35).

Functional characterization of methylated promoters

We then investigated the biological functions and pathways associated with genes having methylated promoters, and therefore likely to be repressed in ESCs or EpiSCs. We selected genes containing highly methylated promoters in EpiSCs or ESCs, that is, those with a read density of at least 20, which corresponds to the median of the read density distribution (Fig. 1C and Supplementary Table S3), resulting in 1,528 genes for ESCs and 2,151 for EpiSCs. Gene ontology analysis using DAVID showed only two terms associated with ESC specific methylation: transmembrane transport and translation (Fig. 3A). Terms showing up only in EpiSCs concerned response to endogenous or extracellular stimuli. Most terms (14/21) were common to both cell types, such as germ cell development and reproductive function, ion transport, and cell adhesion. In addition, two

A

	MP EpiSC1	MP EpiSC2	MP EpiSC3	MP ESC	T EpiSC1	T EpiSC2	T EpiSC3	T ESC
MP_EpiSC1	1.00	0.68	0.85	0.51	**-0.23**			
MP_EpiSC2	0.68	1.00	0.61	0.31		**-0.08**		
MP_EpiSC3	0.85	0.61	1.00	0.57			**-0.28**	
MP_ESC	0.51	0.31	0.57	1.00				**-0.35**
T_EpiSC1	**-0.23**				1.00	0.99	0.98	0.90
T_EpiSC2		**-0.08**			0.99	1.00	0.99	0.91
T_EpiSC3			**-0.28**		0.98	0.99	1.00	0.90
T_ESC				**-0.35**	0.90	0.91	0.90	1.00

B

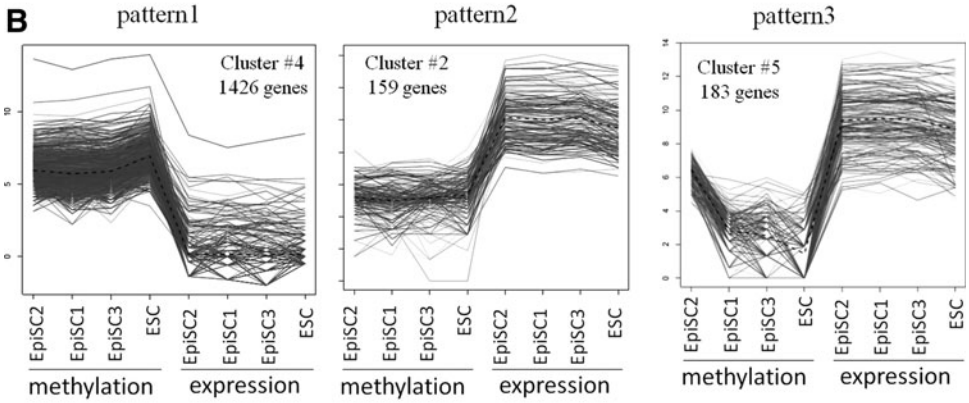

C

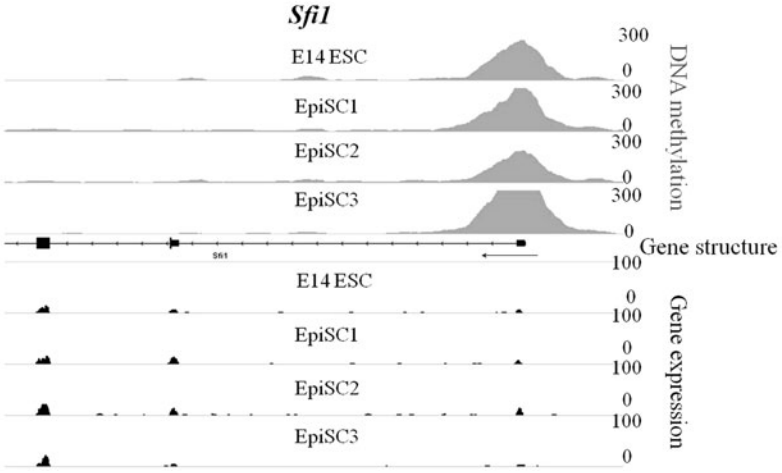

FIG. 2. Relationships between promoter methylation and gene expression. **(A)** Correlation coefficients between DNA methylation on promoters (MP) and expression data (T). **(B)** Three main clusters (Qt-clust) illustrating the relation between promoter methylation and gene expression. **(C)** Example of a gene following pattern 1.

Kegg pathways were common to ESCs and EpiSCs: neuroactive ligand-receptor interaction and ribosome. Interestingly, there were always more genes with methylated promoters in EpiSCs belonging to these common terms than for ESCs. This suggests that the repression of certain biological processes initiated in ESCs was amplified in EpiSCs. To further document this trend, we selected genes belonging to two well-represented categories, ''sexual reproduction'' and ''gamete generation'' and compared the levels of both DNA methylation and gene expression. Most genes belonging to these categories displayed much lower expression, while higher DNA methylation, in EpiSCs as compared with ESCs (Fig. 3B). It has been reported that several germ cell markers are downregulated in EpiSCs compared with ESCs including *Piwil2* and *Nr0b1* [6]. We now show that both genes are hypermethylated in EpiSCs compared with ESCs (Fig. 3C).

Among genes showing hypermethylated promoters in EpiSCs, *Dppa3* (*Stella*) and *Zfp42* (*Rex1*) have been shown to be methylated at their promoters and their expression repressed in EpiSCs, in contrast to ESCs ([9,36], and Supplementary Fig. S3B for Zfp42). Interestingly, also *Tbx3,* another ''naïve'' gene important for ESC maintenance [37], is specifically methylated in EpiSC, with concordant lower

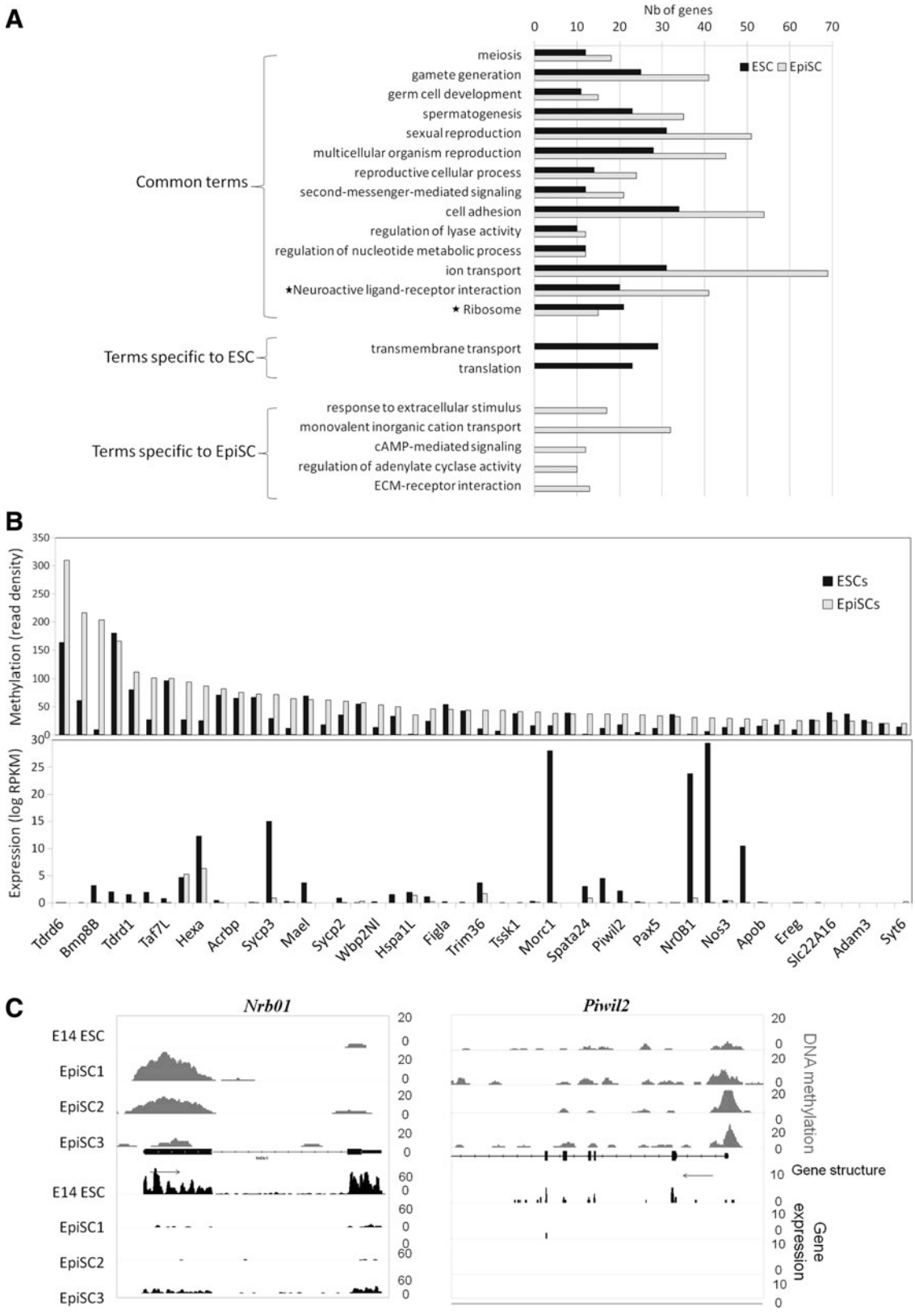

FIG. 3. Functional annotation of methylated promoters. **(A)** GO terms associated with promoters methylated (read density >20) in EpiSCs and in ESCs, according to DAVID analysis (P-value $\leq 1\%$). The *indicate KEGG pathways. **(B)** Plots comparing methylation and expression of the 49 genes associated with the union of ''gamete generation'' and ''sexual reproduction'' GO terms. **(C)** IGV browser view of two germline and ESC-specific genes, *Nr0b1* and *Piwil2*, showing the de novo methylation and loss of gene expression in EpiSCs compared to ESCs.

expression in EpiSCs as compared with ESCs (Supplementary Fig. S3C). The zygotic promoter of Dnmt3l, which controls its expression during preimplantation stages, was also methylated in EpiSCs (Supplementary Fig. S3D), as is the case in the postimplantation epiblast [16]. Expression of these genes are quickly downregulated during conversion of ESCs to EpiSCs [38]; (see below). Together, our data suggest that DNA methylation at promoters in EpiSCs contributes to the regulation of genes that are differentially expressed in naïve versus primed pluripotent cells.

Identification and characteristics of differentially methylated promoters

To identify differentially methylated regions (DMRs) between ESCs and EpiSCs, we selected regions displaying a read density ratio of at least three between the two cell types with a minimum of 20 reads for the category with the highest count. This analysis was performed on the whole dataset and revealed 1,226 hypermethylated regions specific for ESCs and twice more (2,852) for EpiSCs. Among these DMRs, 724 (25%) are annotated as promoters specifically hypermethylated in EpiSCs, and only 58 (5%) are promoters that are hypermethylated specifically in ESCs, again illustrating that promoters tend to become hypermethylated in EpiSCs (Fig. 4A). Promoters hypermethylated in EpiSCs were found associated with molecular transport, metabolism, signaling, and nervous system development (Supplementary Fig. S3A). The same analysis performed on the promoters that are hypermethylated in ESCs did not yield significant results because of the low number of genes.

When CpG density was taken into account, the proportion of each category was identical for the small set of hypermethylated promoters in ESCs, compared to that of all methylated promoters (Fig. 4B). By contrast, only ICPs and HCPs were represented among promoters hypermethylated in EpiSCs, the latter being the most abundant and clearly overrepresented when compared to the population of all methylated promoters (78% compared to 35%).

Using published ChIP-seq data on histone modifications in ESCs [39,40], we determined that half of the hypermethylated promoters in EpiSCs were associated with bivalent domains (H3K4me3/H3K27me3) in ESCs (Fig. 4C), while the remaining were mainly associated with H3K4me3. Hence, these (bivalent) genes are likely stably silenced in EpiSCs by deposition of dense methylation at their promoters.

To validate the current MethylCap-seq, six DMRs in promoters were selected and assessed by bisulfite sequencing. The six genes were chosen among those with hypermethylated promoter and no expression in EpiSCs, and associated with bivalent promoters in ESCs (Supplementary Fig. S4). Of these, *Abcb1*a is a membrane transporter whereas the others are involved in development [41]. *Chrna3*, *Cspg4*, *Daam2*, and *Gfra3* play roles in nervous system development [42–46], while *Aebp1* is required for smooth muscle formation [47–50]. We verified the low level of DNA methylation in two different ESC lines, which contrasted with the high DNA methylation level (90%–98% methylated CpGs) in two EpiSC lines (Fig. 4D). These results highly correlated with the MethylCap-seq data.

To better understand the basis of the methylation difference between ESCs and EpiSCs, we assessed the RNA expression of the de novo methyltransferases *Dnmt3a*, *3b*, and *3l*, and the *Tet* enzymes that are involved in active demethylation (Fig. 4E). *Dnmt3a* is expressed at a similar level in the two cell types, whereas *Dnmt3b* expression is about four-fold higher in EpiSCs, while *Dnmt3l* is only expressed in ESCs. Expression of both *Tet1* and *Tet2* is lower in EpiSCs, while *Tet3* expression is low in both cell types. The protein level of both DNMT3A and 3B was evaluated by western-blotting (Fig. 4F, G). In good correlation with transcript level, DNMT3B is greater than eightfold higher in EpiSCs compared with ESCs. As expected, the total quantity of DNMT3A was similar in both cell types, but distributed over two different isoforms: the lower band of $\sim$75 kDa corresponding to DNMT3A isoform 2 (DNMT3A2, [51]) is higher in ESCs, whereas the higher band ($\sim$100 kDa; DNMT3A1) appeared only in EpiSCs and accounted for about half of the total quantity of DNMT3A in these cells. In conclusion, compared with ESCs, EpiSCs have more abundant DNMT3B and DNMT3A1, whereas *Dnmt3l*, *Tet1*, and *Tet2* are much lower.

Dynamics and role of DNA methylation changes during conversion of ESCs into cEpiSCs

EpiSCs can be obtained directly in vitro from ESCs by applying EpiSC culture conditions to the ESCs (cEpiSCs, [9,10]. In cEpiSCs harvested 13–15 passages after conversion, the level of expression of the *Dnmt3* and *Tet* genes is very similar to that of embryo-derived EpiSCs

FIG. 4. EpiSCs tend to contain hypermethylated promoters. **(A)** Pie charts showing the classification of hypermethylated regions in ESCs (read density ratio ESC/EpiSC >3) and hypermethylated in EpiSCs (read density ratio EpiSC/ESC >3). The number of DMRs is indicated below the pies. ESC and EpiSC distribution differ significantly (Chi-squared test, P-value $< 10^{-53}$). **(B)** Classification of all methylated (read density $\neq 0$) and differentially methylated promoters as HCP, ICP, and LCP. Hypermethylated promoters in EpiSCs are significantly enriched in HCP (Chi-squared test, P-value $< 10^{-76}$). **(C)** Classification of all promoters (read density in EpiSC $\neq 0$) and differentially methylated promoters in EpiSC (ratio EpiSC/ESC >3) according to their association in ESC with H3K4me3 (*gray*), H3K27me3 (*white*), bivalent (H3K4me3 + H3K27me3, *hatched*) or neither mark (*black*). Hypermethylated promoters are significantly different from all promoters (Chi-squared test, P-value $< 10^{-22}$). **(D)** Validation of differential methylation between EpiSCs and ESCs. The class of each promoter according to their CpG content is indicated. *Circles* represent CpG nucleotides either methylated (*closed*) or unmethylated (*open*). **(E)** Gene expression of DNA methylation modifying enzymes in ESCs and EpiSCs determined by RT-qPCR. Error bars represent SEM of three different cell lines. **(F, G)** Western blots showing the protein level of Dnmt3a and Dnmt3b in ESCs and EpiSCs. The average quantity relative to Actin is shown on the *right*. Error bars represent SEM of two (ESCs) to three (EpiSCs) different cell lines. *in **E, F**: $P < 0.05$, Mann–Whitney U test.

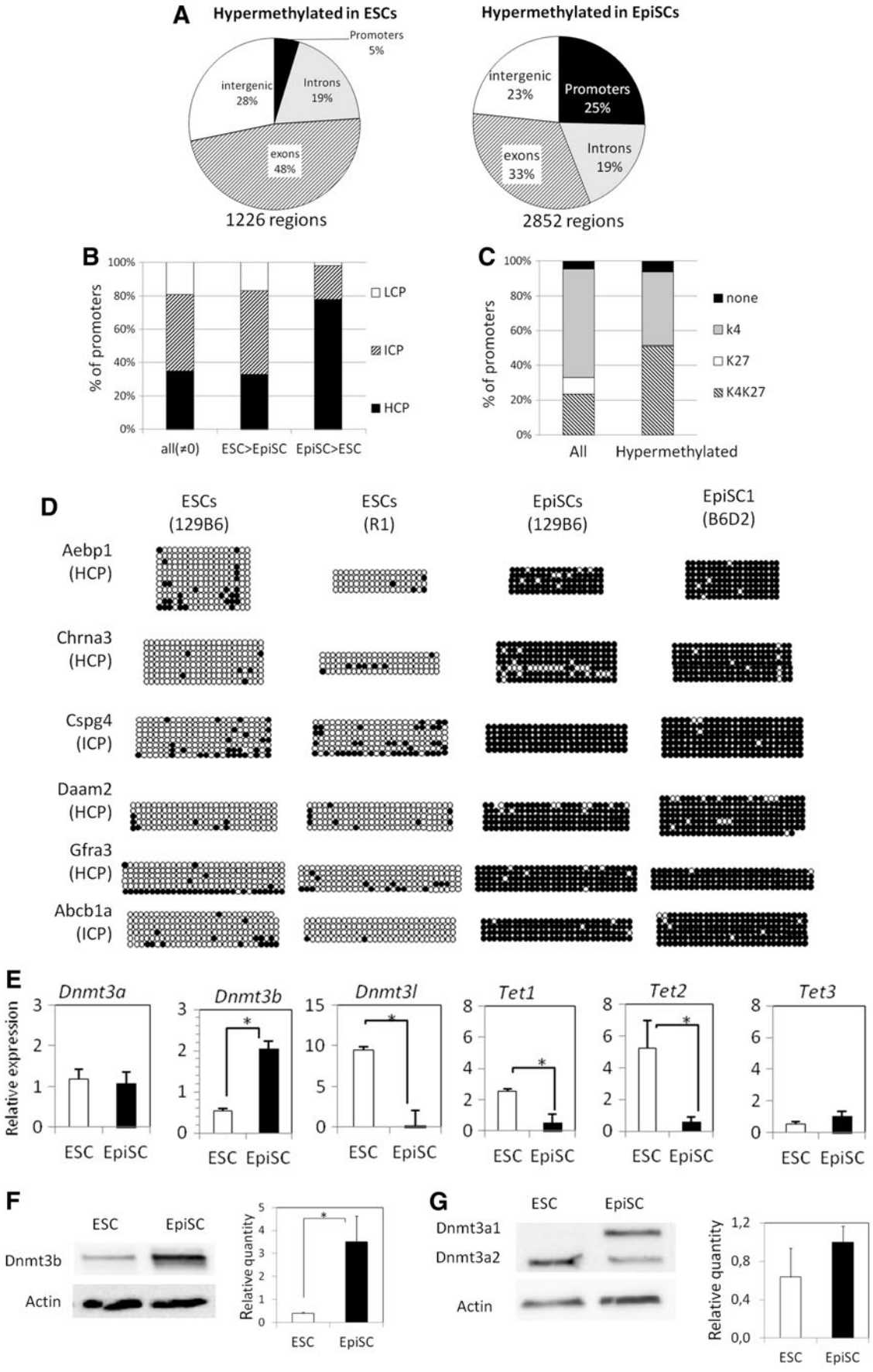
A
Hypermethylated in ESCs
Promoters 5%
Introns 19%
exons 48%
intergenic 28%
1226 regions
Hypermethylated in EpiSCs
Promoters 25%
Introns 19%
exons 33%
intergenic 23%
2852 regions
B
% of promoters
LCP
ICP
HCP
all(≠0)
ESC>EpiSC
EpiSC>ESC
C
% of promoters
none
k4
K27
K4K27
All
Hypermethylated
D
ESCs (129B6)
ESCs (R1)
EpiSCs (129B6)
EpiSC1 (B6D2)
Aebp1 (HCP)
Chrna3 (HCP)
Cspg4 (ICP)
Daam2 (HCP)
Gfra3 (HCP)
Abcb1a (ICP)
E
Relative expression
Dnmt3a
Dnmt3b
Dnmt3l
Tet1
Tet2
Tet3
ESC EpiSC
F
ESC EpiSC
Dnmt3b
Actin
Relative quantity
G
ESC EpiSC
Dnmt3a1
Dnmt3a2
Actin
Relative quantity

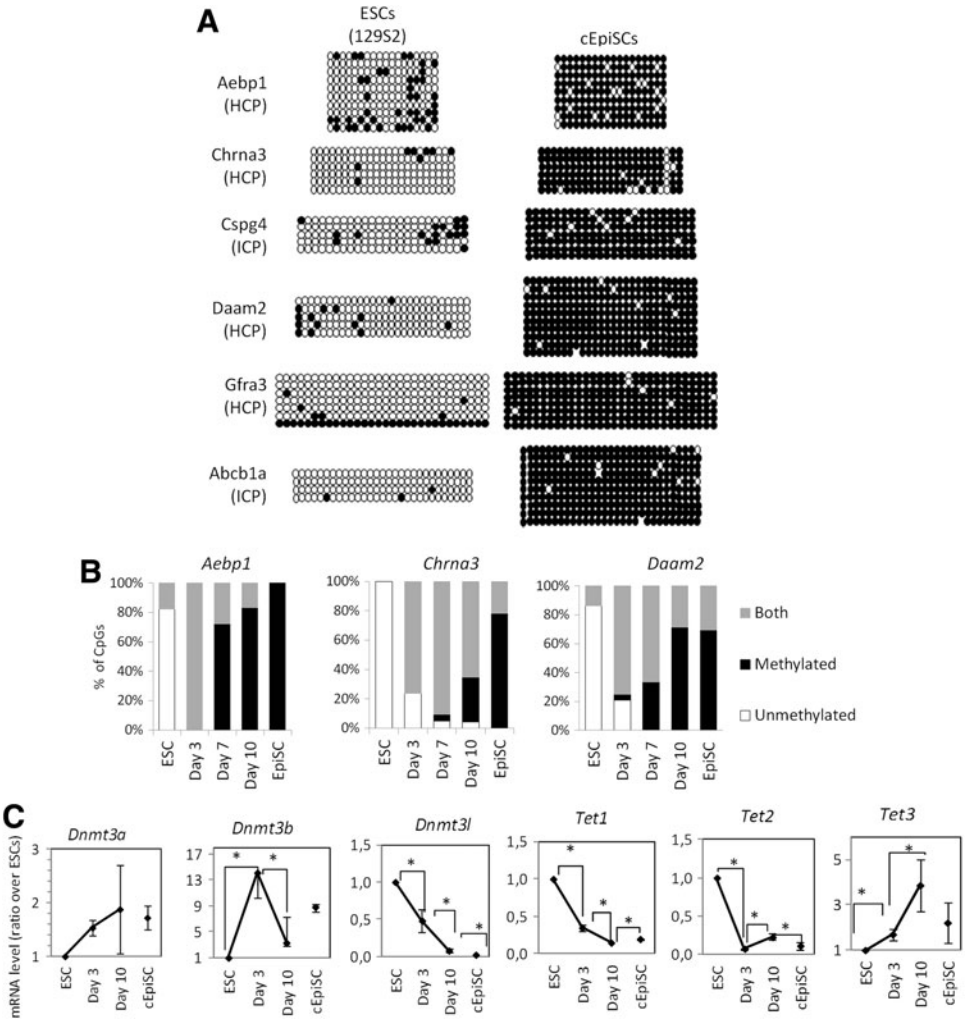

FIG. 5. Characterization of ESC conversion into cEpiSC. **(A)** Changes of methylation in the six promoters assessed by bisulfite-sequencing during conversion of ESCs into cEpiSCs. **(B)** Changes in the CpG level of methylation in the promoter of *Aebp1*, *Chrna3*, and *Daam2* during the conversion process. Genomic DNA after bisulfite conversion was directly sequenced. Each CpG has been classified according to the presence of a C (methylated), a T (unmethylated), or a polymorphism meaning heterogeneity between the two forms in the cell population (both). **(C)** Changes in expression of DNA methylation modifying enzymes, during the conversion of ESCs determined by RT-qPCR. Bars represent SEM of three independent experiments. $*P < 0.05$, Mann–Whitney U test.

(Supplementary Fig. S5A). In line with this, the pattern of DNA methylation of embryo-derived EpiSCs was also correctly apposed in these cEpiSC: a very similar, dense methylation was observed in both EpiSCs and cEpiSCs (88%–98%) for the six promoters described above (Fig. 5A; see Fig. 4D for comparison). During conversion, colonies with an EpiSC-like morphology first appeared at day 6 (Supplementary Fig. S5B), while changes in gene expression levels of ESC markers such as *Klf4 and Dppa3*, or the upregulation of the EpiSC marker *Fgf5*, occur as early as at day 3 (Supplementary Fig. S5C). We therefore asked when the de novo methylation occurred during the conversion. To this end, bisulfite sequencing was performed on *Aebp1* and *Chrna3* promoters at day 3, 7, and 10 of conversion (Fig. 5B). In parallel, we also examined the dynamics of expression of the *Dnmt3* and the *Tet* genes (Fig. 5C). At day 3, sequence polymorphism was present at most CpG loci (Fig. 5B), indicating that de novo methylation had already started, in accordance with the early upregulation of *Dnmt3b* and the downregulation of *Tet1* and *Tet2*. *Dnmt3l*, on the other hand, was quickly downregulated and, intriguingly, *Tet3* was transiently upregulated during conversion, although remaining at low level. Altogether, our results show that DNA hypermethylation at promoters occurs early in the transition from ESCs to EpiSCs.

Reprogramming of DNA methylation during reversion of EpiSCs to ESCs

As DNA methylation is considered to be a stable epigenetic mark, we next asked whether reprogramming of EpiSCs toward ESCs would efficiently reverse methylation at promoters. The DNA methylation status at the six promoters as mentioned above was analyzed in rESCs harvested 11–13 passages after the start of reversion by transferring the EpiSCs onto feeders in LIF-containing medium [9]. Although DNA methylation was largely reduced, all six genes displayed a higher level of DNA methylation at their promoters in the rESCs as compared with the embryo-derived ESCs (Fig. 6A). Remarkably, we observed heterogeneity between clones, representing different alleles in the population: some were highly methylated while others were unmethylated as is the case for *Daam2*. This is in contrast with embryo-derived ESCs in which the DNA methylation level at each allele was quite similar (see Fig. 4D for comparison). We verified that the level of expression of *Dnmt3s* and *Tets* was correctly reprogrammed in rESCs compared with embryo-derived ESCs (Supplementary Fig. S6).

Bisulfite sequencing of individual alleles after cloning does not allow distinguishing between allelic heterogeneity

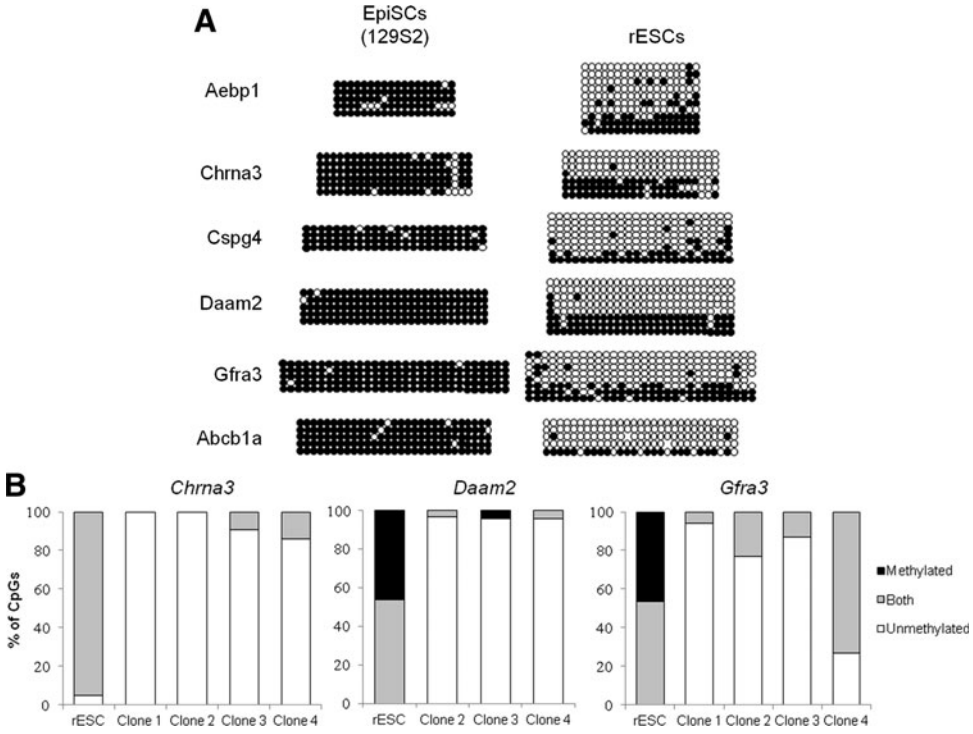

FIG. 6. Characterization of EpiSC reversion into rESC. **(A)** Changes of methylation in the six promoters assessed by bisulfite-sequencing during reversion of EpiSCs into rESCs. **(B)** CpG level of methylation in the promoter of *Chrna3*, *Daam2*, and *Gfra3* after clonal expansion of rESCs. As in Fig. 5B, each CpG is classified as methylated, unmethylated, or polymorphic (both) in the cell population.

within cells or among the cell population, as linkage information between the different fragments is lost. Therefore, we grew four rESC clones originating from single rESCs and determined the methylation status of the three promoters showing the highest methylation heterogeneity (*Chrna3*, *Daam2*, and *Gfra3*; Fig. 6B). Surprisingly, clones were now mostly demethylated, with the notable exception of *Gfra3* for clone 4, which still exhibited some methylated CpGs. These results indicate that DNA methylation is stable and resistant to reprogramming although further passages and severe selection by sub-cloning is able to almost, but not totally, erase this epigenetic memory.

Comparison of methylated promoters in EpiSC compared to the epiblast

It has been reported that the DNA methylation signature at promoters in ESCs is closer to the early postimplantation epiblast than to the ICM that they are derived from [12]. We now asked how promoter methylation in EpiSCs compared with that of their in vivo counterpart. We isolated epiblasts from early (E6.5) or late (E7) gastrulating embryos and performed bisulfite sequencing on the six promoters that were strongly methylated in EpiSCs. The DNA methylation level in epiblasts was very low at the two stages and even lower than the level of methylation observed in ESCs for *Aebp1*, *Cspg4*, and *Gfra3* (Fig. 7A and Supplementary Fig. S7).

To perform this analysis at a global scale, we compared our data with the publicly available dataset of promoter methylation on E6.5 epiblasts obtained by MedIP arrays [12] after selection of promoters common to the two study (2,610 promoters; Supplementary Table S4 and Fig. 7B). The majority of promoters (77%, 1,861/2,416) that were methylated in EpiSCs (at least 10 reads) had a low level of methylation in epiblast (log2ratio < 0.3). Conversely, very few promoters with low level of methylation in EpiSCs were methylated in the epiblast (8%, 15/194). Methylation at these promoters is therefore unique to EpiSCs, and does not recapitulate the methylation status of the epiblast stage they are derived from. The expression level of *Dnmt3s* and *Tets* in epiblast and EpiSCs could not explain this difference in methylation deposition, as these enzymes were similarly expressed, except for *Dnmt3b*, which is even higher expressed in the epiblast (Fig. 7C).

To get insight into the kinetic of this methylation process during EpiSC derivation, day 6.5 epiblasts were explanted in culture and outgrowths collected at different time points. Bisulfite conversion followed by direct sequencing was performed on three representative promoters, *Aebp1*, *Chrna3*, and *Daam2* (Fig. 7D). Completely methylated CpGs started to appear as early as day 2 for *Aebp1* and before day 9 for *Chrna3*. For *Aebp1*, it reached the level of established EpiSCs within 9 days. Such kinetic is not in favor of a slow deposition of methylation along passages in culture but rather suggests that the removal of the epiblast from its in vivo environment and/or the culture conditions may have released constraints that prevent promoter hypermethylation within the embryo.

Lastly, to gain insight into the functional consequence of the differential DNA methylation, we asked whether the difference in promoter DNA methylation between EpiSCs and epiblast cells translated into differences in expression of the corresponding genes. Using available microarray data on expression in the epiblast [32], we determined the expression status (expressed or not expressed) of genes in the epiblast with contain hypermethylated promoters in EpiSCs (reads ≥ 20) (Fig. 7E and Supplementary Table S4). Most

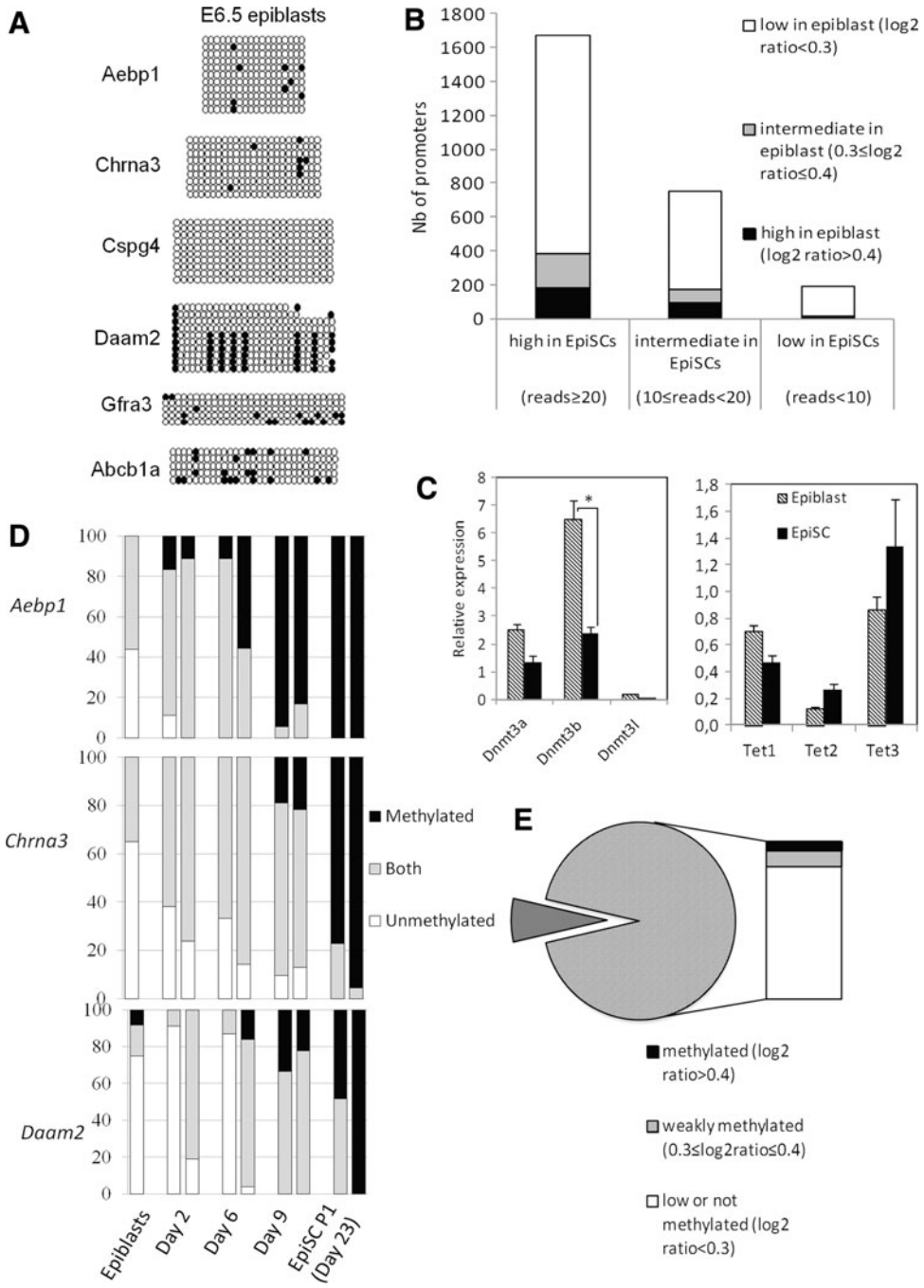

FIG. 7. Differential methylation in embryo-derived pluripotent cells and in the epiblast. **(A)** Methylation status in the epiblast (E6.5). **(B)** Comparison of methylation in promoters common to Borgel et al. [12]) and our study. Promoters were classified according to their mean methylation status in EpiSCs and each category further separated according to their methylation values in E6.5 epiblasts. **(C)** Gene expression of DNA methylation modifying enzymes in E6.5 epiblast and EpiSCs determined by RT-qPCR. Bars represent SEM. $*P < 0.05$, Mann–Whitney U test. **(D)** Changes in the CpG level of methylation in the promoter of *Aebp1*, *Chrna3*, and *Daam2* during derivation of EpiSCs. Genomic DNA after bisulfite conversion was directly sequenced and the status of the CpGs was indicated as in Figs. 5 and 6. **(E)** Expression status in the epiblast of genes that contain methylated promoters in EpiSCs.

genes (93%, 554/593) were not expressed in the epiblast, although being largely unmethylated. This suggests that for a large set of genes that are repressed in both the epiblast and their in vitro counterparts (the EpiSCs), the epigenetic mechanism of repression is different.

Discussion

We have compared the DNA methylome of EpiSCs to that of ESCs and to their tissue of origin, the post-implantation epiblast. ESCs and EpiSCs have similar methylation levels and a similar distribution of methylation within the different genomic regions. However, several features distinguish the two cell types, in particular the fact that there are significantly more regions specifically methylated in EpiSCs as compared to ESCs, a large part of those being hypermethylated HCP promoters. These promoters are mostly associated with either a bivalent signature (H3K4me3 and H3K27me3) or an active H3K4me2/me3 mark in the ESCs [39,40]. Furthermore, our study suggests that the promoter methylation pattern is quickly established during the in vitro conversion of ESCs into EpiSCs.

To further validate our findings on an independent dataset, we re-examined the MeDIP-seq data generated by Senner et al. [21]. This analysis yielded the same results as with our dataset: a larger set of hypermethylated, high-CpG

content promoters is present in EpiSCs compared with ESCs, and these promoters are associated with a bivalent signature in ESCs (Supplementary Fig S8A, B). GO term analysis of methylated promoters in both cell types also shows overlap with our analysis (see Fig. 3A), with a prominent targeting of methylation toward germline associated promoters (Supplementary Fig. S8C). In addition, a recent report by Hackett et al. shows an increase of methylcytosine at promoters in EpiSC [52]. Together, these two independent analyses performed on ESC and EpiSCs of different origins with different profiling techniques show that the epigenome of the primed EpiSCs clearly differ from that of the naïve ESCs.

The differences in promoter methylation in the two pluripotent cell types reported here are well correlated with the differences in expression of the enzymes involved in the control of DNA methylation. We show that Dnmt3b is more abundant in EpiSCs compared with ESCs, which in particular could explain the increased deposition of methylation at promoters of germline genes [53]. The expression of the two main Tet enzymes involved in active demethylation and present in ESCs, *Tet1* and *Tet2*, are largely downregulated in EpiSCs. Interestingly, TET1 has been suggested to help in maintaining a demethylated state at bivalent promoters [54,55]. Dnmt3l, a cofactor of Dnmt3a/3b, also rapidly decreases during ESC-EpiSC conversion and remains low in EpiSCs. A recent study have shown that DNMT3L interacts with PRC2, the polycomb complex that tri-methylates H3K27, which helps in maintaining the bivalent domains free of DNA methylation by preventing their access by DNMT3A/3B [56]. Although the total quantity of DNMT3A remains constant in EpiSCs and ESCs, an additional splicing isoform, DNMT3A1, is present in EpiSCs [51]. Interestingly, this isoform is also upregulated upon retinoic acid ESC differentiation and exhibits distinct gene targets [57]. Altogether these data provide a functional explanation for the preferential deposition of DNA methylation in EpiSC at sites that show bivalent histone marks in ESCs.

Our study indicates that ESCs obtained by reversion of EpiSCs show persistent methylation at some promoters, which is very difficult to erase. Even after extended culture and stringent selection, a residual methylation apparently persists at some alleles and some CpGs. Culture of the revertant cells at clonal density excludes the presence of any residual EpiSCs that would die in our assay when passaged as single cells [3]. Persistence of residual methylation has been previously observed in somatic cells reprogrammed using defined factors (iPSCs). It was recognized as an epigenetic memory, which could be erased at high passages [58–60]. Reverted ESCs generated using the same protocol as ours have been shown to be transcriptionally similar to ESCs, even after a few passages, and able to give rise to germline-competent chimeras [9], suggesting that the residual methylation does not impair the establishment of naïve pluripotency. Reversion of EpiSC to ESCs has been successfully used as a model system to seek for factors that facilitate reprogramming [61]. We propose that a quick and complete erasure of DNA methylation at promoters would be a good criterion for reprogramming efficiency.

The comparison of our dataset of methylated promoters in EpiSCs with the dataset on epiblast cells [12] revealed that many methylated promoters in EpiSCs are poorly methylated in the epiblast. Hence, hypermethylation at promoters appears also to be a distinguishing feature of EpiSCs compared to their in vivo counterpart. During epiblast culture, we observed a rapid de novo methylation at the tested promoters, within 3 days, similar to deposition of methylation during conversion of ESCs into EpiSCs. Although the difference in promoter methylation in epiblast and EpiSC does not have an immediate consequence in terms of gene expression differences, it nevertheless implies that the epigenetic regulation of EpiSCs differs from that of their tissue of origin, the epiblast. It is possible that in vivo the deposition of methylation is controlled by external factors that are relieved when the epiblast is explanted in vitro without any surrounding tissues. Indeed, when the epiblast is dissociated into single cells and cultured on feeders with LIF and serum-containing medium, both *Rex1* and *Dppa3* promoters, initially demethylated in the epiblast, become transiently methylated, as they are in EpiSCs [9]. Culture conditions used for EpiSCs required two active signaling pathways, Activin/Nodal and FGF [29,62,63], which may be involved in the stimulation of the hypermethylation in EpiSCs. Interestingly, when ESCs are transferred from serum-containing medium to serum-free medium containing MEK and GSK3 inhibitors, they become extensively demethylated [19,20]. This is also the case for reverted ESCs, which become more demethylated when grown in the same serum-free conditions (data not shown). Several studies have highlighted a complex crosstalk between FGF signaling, Prdm14, Dnmt3b, and Tet that could play an inductive role in this process [19,64,65]. In vivo, FGF signaling activity as revealed by phosphorylated Erk1/2 is low in the pregastrulation epiblast cells but becomes activated upon derivation in the presence of FGF2-containing medium [62,66]. As shown in this study, the conversion of ESCs into EpiSCs provides an excellent system to further decipher the role of these various components in the regulation of DNA methylation.

In conclusion, our study shows that EpiSCs have a specific DNA methylome signature, in particular at promoters. It differs from both ESCs and from the epiblast they originate from, and cannot be easily erased by reprogramming EpiSCs to a more naïve ESC-like state through modulation of the culture conditions. The rapid molecular and epigenetic changes during the first days of ESC-to-EpiSC conversion make it an interesting system to further study the role of DNA methylation in the transition from naïve to a primed state of pluripotency.

Acknowledgments

We thank E.M. Janssen-Megens and Y. Tan for technical support with sequencing. Femke Simmer and Arjen Brinkman helped with the analysis of MethylCap-seq data. We are grateful to Hélène Jammes and Sylvie Ruffini for technical help in bisulfite sequencing and western-blotting, respectively. Many thanks to Gabriel Brons for the derivation of 129S2 EpiSC. The research leading to these results has received funding from PluriSys (FP7/2009: 223485) and by ANR Programme Investissements d'Avenir REVIVE. ACV and MT are recipients of a PhD fellowship from DIM STEM Pole and DIM Biotherapies Ile-de-France. HM is supported by a grant from The Netherlands Organization for Scientific

Research (NWO-VIDI 864.12.007). ASB was part sponsored by the British Heart Foundation (FS/12/37/29516).

Author Disclosure Statement

No financial competing interest exists.

References

1. Hutchins AP, SH Choo, TK Mistri, M Rahmani, CT Woon, CK Ng, R Jauch and P Robson. (2013). Co-motif discovery identifies an Esrrb-Sox2-DNA ternary complex as a mediator of transcriptional differences between mouse embryonic and epiblast stem cells. Stem Cells 31:269–281.
2. Nichols J and A Smith. (2012). Pluripotency in the embryo and in culture. Cold Spring Harb Perspect Biol 4:a008128.
3. Brons IGM, LE Smithers, MWB Trotter, P Rugg-Gunn, B Sun, SM Chuva de Sousa Lopes, SK Howlett, A Clarkson, L Ahrlund-Richter, RA Pedersen and L Vallier. (2007). Derivation of pluripotent epiblast stem cells from mammalian embryos. Nature 448:191–195.
4. Chenoweth JG, RDG McKay and PJ Tesar. (2010). Epiblast stem cells contribute new insight into pluripotency and gastrulation. Dev Growth Differ 52:293–301.
5. Nichols J and A Smith. (2009). Naive and primed pluripotent states. Cell Stem Cell 4:487–492.
6. Tesar PJ, JG Chenoweth, FA Brook, TJ Davies, EP Evans, DL Mack, RL Gardner and RDG McKay. (2007). New cell lines from mouse epiblast share defining features with human embryonic stem cells. Nature 448:196–199.
7. Huang Y, R Osorno, A Tsakiridis and V Wilson. (2012). In Vivo differentiation potential of epiblast stem cells revealed by chimeric embryo formation. Cell Reprog 2:1571–1578.
8. Ying QL, J Nichols, I Chambers and A Smith. (2003). BMP induction of Id proteins suppresses differentiation and sustains embryonic stem cell self-renewal in collaboration with STAT3. Cell 115:281–292.
9. Bao S, F Tang, X Li, K Hayashi, A Gillich, K Lao and MA Surani. (2009). Epigenetic reversion of post-implantation epiblast to pluripotent embryonic stem cells. Nature 461:1292–1295.
10. Guo G, J Yang, J Nichols, JS Hall, I Eyres, W Mansfield and A Smith. (2009). Klf4 reverts developmentally programmed restriction of ground state pluripotency. Development 136:1063–1069.
11. Zhou HY, WL Li, SY Zhu, JY Joo, JT Do, W Xiong, JB Kim, K Zhang, HR Scholer and S Ding. (2010). Conversion of mouse epiblast stem cells to an earlier pluripotency state by small molecules. J Biol Chem 285:29676–29680.
12. Borgel J, S Guibert, Y Li, H Chiba, D Schubeler, H Sasaki, T Forne and M Weber. (2010). Targets and dynamics of promoter DNA methylation during early mouse development. Nat Genet 42:1093–1100.
13. Smith ZD, MM Chan, TS Mikkelsen, H Gu, A Gnirke, A Regev and A Meissner. (2012). A unique regulatory phase of DNA methylation in the early mammalian embryo. Nature 484:339–344.
14. Mikkelsen TS, J Hanna, X Zhang, M Ku, M Wernig, P Schorderet, BE Bernstein, R Jaenisch, ES Lander and A Meissner. (2008). Dissecting direct reprogramming through integrative genomic analysis. Nature 454:49–55.
15. Okano M, DW Bell, DA Haber and E Li. (1999). DNA methyltransferases Dnmt3a and Dnmt3b are essential for de novo methylation and mammalian development. Cell 99:247–257.
16. Guenatri M, R Duffie, J Iranzo, P Fauque and D Bourc'his. (2013). Plasticity in Dnmt3L-dependent and -independent modes of de novo methylation in the developing mouse embryo. Development 140:562–572.
17. Hirasawa R and H Sasaki. (2009). Dynamic transition of Dnmt3b expression in mouse pre- and early post-implantation embryos. Gene Exp Patterns 9:27–30.
18. Hu Y-G, R Hirasawa, J-L Hu, K Hata, C-L Li, Y Jin, T Chen, E Li, M Rigolet, et al. (2008). Regulation of DNA methylation activity through Dnmt3L promoter methylation by Dnmt3 enzymes in embryonic development. Hum Mol Gen 17:2654–2664.
19. Leitch HG, KR McEwen, A Turp, V Encheva, T Carroll, N Grabole, W Mansfield, B Nashun, JG Knezovich, et al. (2013). Naive pluripotency is associated with global DNA hypomethylation. Nat Struct Mol Biol 20:311–316.
20. Habibi E, AB Brinkman, J Arand, LI Kroeze, HH Kerstens, F Matarese, K Lepikhov, M Gut, I Brun-Heath, et al. (2013). Whole-genome bisulfite sequencing of two distinct interconvertible DNA methylomes of mouse embryonic stem cells. Cell Stem Cell 13:360–369.
21. Senner CE, F Krueger, D Oxley, S Andrews and M Hemberger. (2012). DNA methylation profiles define stem cell identity and reveal a tight embryonic-extraembryonic lineage boundary. Stem Cells 30:2732–2745.
22. Bock C, EM Tomazou, AB Brinkman, F Muller, F Simmer, H Gu, N Jager, A Gnirke, HG Stunnenberg and A Meissner. (2010). Quantitative comparison of genome-wide DNA methylation mapping technologies. Nat Biotechnol 28: 1106–1114.
23. Huang DW, BT Sherman and RA Lempicki. (2008). Systematic and integrative analysis of large gene lists using DAVID bioinformatics resources. Nat Protocols 4:44–57.
24. Huang DW, BT Sherman and RA Lempicki. (2009). Bioinformatics enrichment tools: paths toward the comprehensive functional analysis of large gene lists. Nucl Acids Res 37:1–13.
25. Anders S and W Huber. (2010). Differential expression analysis for sequence count data. Genome Biol 11:R106.
26. Leisch F. (2006). A toolbox for -centroids cluster analysis. Comput Stat Data Anal 51:526–544.
27. Bryja V, S Bonilla, L Cajanek, CL Parish, CM Schwartz, Y Luo, MS Rao and E Arenas. (2006). An efficient method for the derivation of mouse embryonic stem cells. Stem Cells 24:844–849.
28. Jouneau A, C Ciaudo, O Sismeiro, V Brochard, L Jouneau, S Vandormael-Pournin, JY Coppee, Q Zhou, E Heard, C Antoniewski and M Cohen-Tannoudji. (2012). Naive and primed murine pluripotent stem cells have distinct miRNA expression profiles. RNA 18:253–264.
29. Maruotti J, XP Dai, V Brochard, L Jouneau, J Liu, A Bonnet-Garnier, H Jammes, L Vallier, IG Brons, et al. (2010). Nuclear transfer-derived epiblast stem cells are transcriptionally and epigenetically distinguishable from their fertilized-derived counterparts. Stem Cells 28:743–752.
30. Dupont JM, J Tost, H Jammes and IG Gut. (2004). De novo quantitative bisulfite sequencing using the pyrosequencing technology. Anal Biochem 333:119–127.
31. Bock C, S Reither, T Mikeska, M Paulsen, J Walter and T Lengauer. (2005). BiQ Analyzer: visualization and quality control for DNA methylation data from bisulfite sequencing. Bioinformatics 21:4067–4068.

32. Kojima Y, K Kaufman-Francis, JB Studdert, KA Steiner, MD Power, DA Loebel, V Jones, A Hor, G de Alencastro, et al. (2014). The transcriptional and functional properties of mouse epiblast stem cells resemble the anterior primitive streak. Cell Stem Cell 14:107–120.
33. Matarese F, E Carrillo-de Santa Pau and HG Stunnenberg. (2011). 5-Hydroxymethylcytosine: a new kid on the epigenetic block? Mol Syst Biol 7:562.
34. Marks H, T Kalkan, R Menafra, S Denissov, K Jones, H Hofemeister, J Nichols, A Kranz, A Francis Stewart, A Smith and HG Stunnenberg. (2012). The transcriptional and epigenomic foundations of ground state pluripotency. Cell 149:590–604.
35. Weber M, I Hellmann, MB Stadler, L Ramos, S Paabo, M Rebhan and D Schubeler. (2007). Distribution, silencing potential and evolutionary impact of promoter DNA methylation in the human genome. Nat Genet 39:457–466.
36. Hayashi K, SMCdS Lopes, F Tang and MA Surani. (2008). Dynamic equilibrium and heterogeneity of mouse pluripotent stem cells with distinct functional and epigenetic states. Cell Stem Cell 3:391–401.
37. Niwa H, J Miyazaki and AG Smith. (2000). Quantitative expression of Oct-3/4 defines differentiation, dedifferentiation or self-renewal of ES cells. Nat Genet 24:372–376.
38. Hayashi K, H Ohta, K Kurimoto, S Aramaki and M Saitou. (2011). Reconstitution of the mouse germ cell specification pathway in culture by pluripotent stem cells. Cell 146:519–532.
39. Meissner A, TS Mikkelsen, H Gu, M Wernig, J Hanna, A Sivachenko, X Zhang, BE Bernstein, C Nusbaum, et al. (2008). Genome-scale DNA methylation maps of pluripotent and differentiated cells. Nature 454:766–770.
40. Mikkelsen TS, M Ku, DB Jaffe, B Issac, E Lieberman, G Giannoukos, P Alvarez, W Brockman, TK Kim, et al. (2007). Genome-wide maps of chromatin state in pluripotent and lineage-committed cells. Nature 448:553–560.
41. Sawicki WT, M Kujawa, E Jankowska-Steifer, ET Mystkowska, A Hyc and C Kowalewski. (2006). Temporal/spatial expression and efflux activity of ABC transporter, P-glycoprotein/Abcb1 isoforms and Bcrp/Abcg2 during early murine development. Gene Expr Patterns 6:738–746.
42. Atluri P, MW Fleck, Q Shen, SJ Mah, D Stadfelt, W Barnes, SK Goderie, S Temple and AS Schneider. (2001). Functional nicotinic acetylcholine receptor expression in stem and progenitor cells of the early embryonic mouse cerebral cortex. Dev Biol 240:143–156.
43. Kida Y, T Shiraishi and T Ogura. (2004). Identification of chick and mouse Daam1 and Daam2 genes and their expression patterns in the central nervous system. Brain Res Dev Brain Res 153:143–150.
44. Nakaya MA, R Habas, K Biris, WC Dunty, Jr., Y Kato, X He and TP Yamaguchi. (2004). Identification and comparative expression analyses of Daam genes in mouse and Xenopus. Gene Expr Patterns 5:97–105.
45. Nishiyama A, XH Lin, N Giese, CH Heldin and WB Stallcup. (1996). Co-localization of NG2 proteoglycan and PDGF α-receptor on O2A progenitor cells in the developing rat brain. J Neurosci Res 43:299–314.
46. Widenfalk J, A Tomac, E Lindqvist, B Hoffer and L Olson. (1998). GFRalpha-3, a protein related to GFRalpha-1, is expressed in developing peripheral neurons and ensheathing cells. Eur J Neurosci 10:1508–1517.
47. Ith B, J Wei, SF Yet, MA Perrella and MD Layne. (2005). Aortic carboxypeptidase-like protein is expressed in collagen-rich tissues during mouse embryonic development. Gene Expr Patterns 5:533–537.
48. Layne MD, SF Yet, K Maemura, CM Hsieh, M Bernfield, MA Perrella and ME Lee. (2001). Impaired abdominal wall development and deficient wound healing in mice lacking aortic carboxypeptidase-like protein. Mol Cell Biol 21:5256–5261.
49. Kucharova K and WB Stallcup. (2010). The NG2 proteoglycan promotes oligodendrocyte progenitor proliferation and developmental myelination. Neuroscience 166:185–194.
50. Li J, C Klein, C Liang, R Rauch, K Kawamura and AJ Hsueh. (2009). Autocrine regulation of early embryonic development by the artemin-GFRA3 (GDNF family receptor-alpha 3) signaling system in mice. FEBS Lett 583:2479–2485.
51. Chen T, Y Ueda, S Xie and E Li. (2002). A novel Dnmt3a isoform produced from an alternative promoter localizes to euchromatin and its expression correlates with active de novo methylation. J Biol Chem 277:38746–38754.
52. Hackett Jamie A, S Dietmann, K Murakami, TA Down, HG Leitch and MA Surani. (2013). Synergistic mechanisms of DNA demethylation during transition to ground-state pluripotency. Stem Cell Rep 1:518–531.
53. Velasco G, F Hube, J Rollin, D Neuillet, C Philippe, H Bouzinba-Segard, A Galvani, E Viegas-Pequignot and C Francastel. (2010). Dnmt3b recruitment through E2F6 transcriptional repressor mediates germ-line gene silencing in murine somatic tissues. Proc Natl Acad Sci U S A 107:9281–9286.
54. Williams K, J Christensen and K Helin. (2012). DNA methylation: TET proteins—guardians of CpG islands? EMBO Rep 13:28–35.
55. Wu H, AC D'Alessio, S Ito, Z Wang, K Cui, K Zhao, YE Sun and Y Zhang. (2011). Genome-wide analysis of 5-hydroxymethylcytosine distribution reveals its dual function in transcriptional regulation in mouse embryonic stem cells. Genes Dev 25:679–684.
56. Neri F, A Krepelova, D Incarnato, M Maldotti, C Parlato, F Galvagni, F Matarese, HG Stunnenberg and S Oliviero. (2013). Dnmt3L antagonizes DNA methylation at bivalent promoters and favors DNA Methylation at gene bodies in ESCs. Cell 155:121–134.
57. Kotini AG, A Mpakali and T Agalioti. (2011). Dnmt3a1 upregulates transcription of distinct genes and targets chromosomal gene clusters for epigenetic silencing in mouse embryonic stem cells. Mol Cell Biol 31:1577–1592.
58. Chin MH, MJ Mason, W Xie, S Volinia, M Singer, C Peterson, G Ambartsumyan, O Aimiuwu, L Richter, et al. (2009). Induced pluripotent stem cells and embryonic stem cells are distinguished by gene expression signatures. Cell Stem Cell 5:111–123.
59. Buecker C, H-H Chen, JM Polo, L Daheron, L Bu, TS Barakat, P Okwieka, A Porter, J Gribnau, K Hochedlinger and N Geijsen. (2010). A Murine ESC-like state facilitates transgenesis and homologous recombination in human pluripotent stem cells. Cell Stem Cell 6:535–546.
60. Kim K, A Doi, B Wen, K Ng, R Zhao, P Cahan, J Kim, MJ Aryee, H Ji, et al. (2010). Epigenetic memory in induced pluripotent stem cells. Nature 467:285–290.
61. Rais Y, A Zviran, S Geula, O Gafni, E Chomsky, S Viukov, AA Mansour, I Caspi, V Krupalnik, et al. (2013). Deterministic direct reprogramming of somatic cells to pluripotency. Nature 502:65–70.
62. Greber B, G Wu, C Bernemann, JY Joo, DW Han, K Ko, N Tapia, D Sabour, J Sterneckert, P Tesar and HR Scholer.

(2010). Conserved and divergent roles of FGF signaling in mouse epiblast stem cells and human embryonic stem cells. Cell Stem Cell 6:215–226.
63. Vallier L, S Mendjan, S Brown, Z Chng, A Teo, LE Smithers, MW Trotter, CH Cho, A Martinez, et al. (2009). Activin/Nodal signalling maintains pluripotency by controlling Nanog expression. Development 136:1339–1349.
64. Ficz G, TA Hore, F Santos, HJ Lee, W Dean, J Arand, F Krueger, D Oxley, Y-L Paul, et al. (2013). FGF signaling inhibition in ESCs drives rapid genome-wide demethylation to the epigenetic ground state of pluripotency. Cell Stem Cell 13:351–359.
65. Grabole N, J Tischler, JA Hackett, S Kim, F Tang, HG Leitch, E Magnusdottir and MA Surani. (2013). Prdm14 promotes germline fate and naive pluripotency by repressing FGF signalling and DNA methylation. EMBO Rep 14:629–637.
66. Corson LB, Y Yamanaka, KM Lai and J Rossant. (2003). Spatial and temporal patterns of ERK signaling during mouse embryogenesis. Development 130:4527–4537.

Address correspondence to:
Dr. Alice Jouneau
INRA
UMR1198 Biologie du Développement et Reproduction
Jouy-en-Josas F-78350
France

E-mail: alice.jouneau@jouy.inra.fr

Received for publication December 24, 2013
Accepted after revision April 15, 2014
Prepublished on Liebert Instant Online April 16, 2014